Optica Applicata, Vol. XXXVIII, No. 4, 2008

Optimization of two-dimensional photonic crystal waveguides for TE and TM polarizations

MOHAMMAD DANAIE[1, 2, *], AMIR REZA ATTARI[2], MIR MOJTABA MIRSALEHI[2], SASAN NASEH[2]

[1]Electrical Engineering Department, Amirkabir University of Technology, Teheran, Iran

[2]Electrical Engineering Department, Ferdowsi University of Mashhad, Iran

[*]Corresponding author: mdanaie@gmail.com

In this paper, we optimize the geometries of some 2D photonic crystal waveguides to increase their single-mode bandwidths for TE and TM polarizations. Using the Plane Wave Expansion (PWE) method combined with optimization algorithm, we find the local maxima as well as the global maximum. A photonic crystal waveguide geometry is proposed which has a single-mode normalized bandwidth of 41% for TM polarization. This value is about 7% greater than the corresponding value for the commonly used square lattice of dielectric rods in which a row is removed. Also, some waveguide geometries are proposed for TE polarization and it is shown that one of these geometries can provide a single-mode bandwidth of 39%, while the widest bandwidth reported so far for the TE case is 21%. The dielectric material used for both cases is GaAs with a dielectric constant of 11.4.

Keywords: photonic crystal waveguides, photonic bandgaps, optimization.

1. Introduction

Photonic crystals (PCs) are periodic dielectric structures that under certain conditions prohibit the propagation of electromagnetic waves of certain frequency bands. This phenomenon provides the ability of controlling and manipulating the flow of light [1]. Mathematically speaking, PCs can be periodic in one, two or three dimensions. There also exist types which are referred to as slab PCs. Slab PCs are periodic in two dimensions and have a finite thickness in the other dimension. If the thickness is chosen large enough, usually ten times larger than the lattice constant [2], the 3D slab structure can be approximated by a 2D PC, which has the same index profile. It is interesting to mention that there also exists a local optimum thickness which maximizes the bandgap. 2D numerical analysis using effective index in addition to applying a light cone can be used in this case. Either type of mentioned 2D PCs have been implemented and used. In our simulations, we focus our study on the former case.

A 2D PC structure may have a photonic bandgap for TE, TM or both polarizations. Usually, a triangular lattice of dielectric holes with a radius of 0.3*a*, where *a* is the lattice constant, is used for TE polarization and a square lattice of dielectric rods with a radius of 0.2*a* is used for TM polarization. Annular PCs can be used to obtain complete bandgaps [3]. PCs are used to design optical filters, resonators, waveguides, multiplexers, logical gates, etc. [4–6]. Waveguides are realized by introducing a line defect in the PC structure [7]. Since waveguides are the basic elements of optical circuits, it is desired to increase their bandwidths as much as possible.

Since the guiding modes of a waveguide lies within the bandgap of the corresponding PC, having a large bandgap PC is a necessary condition to obtain a large bandwidth waveguide. For TM polarization, a triangular or square lattice of dielectric rods provides a large bandgap [1]. Conventional TM waveguides are realized by removing a row in a square lattice of dielectric rods [1]. For a square lattice of GaAs circular rods with a dielectric constant of 11.4 and a rod radius of 0.19*a*, the obtained waveguide has a relatively large bandwidth of 33.8% when normalized to its mid-frequency. A Kagome lattice of dielectric rods can also provide large bandgaps for TM polarization and can be used for designing single-mode waveguides [8, 9]. However, since the guiding mode is located at higher frequencies, the normalized bandwidth becomes less than the corresponding value for the square lattice of dielectric rods in which one column is removed. Adding a dielectric slab in the square lattice can further increase the bandwidth [10]. As it will be shown in this paper, the best waveguide structure, which provides a large single-mode bandwidth for TM polarization, is a triangular lattice of dielectric rods in which a row of rods is replaced by a dielectric slab.

For TE polarization, a triangular lattice of holes of 0.45*a* radius creates the largest bandgap. However, in order to avoid the structure to become fragile, a radius of 0.3*a* is often used. Unlike TM waveguides, several methods have been proposed in the literature for increasing the bandwidths of TE waveguides [11–13]. These methods try to maximize the bandwidth by optimizing the parameters of the line defect or the adjacent rows assuming other holes to have a radius of 0.3*a*. Combining these methods, a waveguide geometry is obtained which increases the single-mode bandwidth to 21% [14].

In order to have a wide bandwidth waveguide, the parameters of the defect region should be chosen carefully. In this paper, an optimization algorithm is used to obtain the optimum structure. This algorithm searches the space of some predefined input variables and finds the local maxima as well as the global maximum. The 2D PWE method is used to calculate the single-mode bandwidth of waveguides. Here, we show that a combination of a dielectric strip waveguide and a triangular lattice of dielectric rods can provide a better performance than the conventionally used square lattice PCs for TM polarization. Furthermore, we introduce some geometries that nearly double the maximum bandwidth obtained for TE polarization.

The paper is organized as follows. Section 2 describes the optimization algorithm used. The optimization geometries used are described in Section 3, while Section 4

provides the optimization results for TM polarization. In Section 5, we first summarize the methods reported in the literature for increasing the TE waveguides bandwidths and then we present our optimization results for TE waveguides. Finally, Section 6 is devoted to the conclusions.

2. The optimization algorithm

Several algorithms can be used for optimization, such as genetic algorithms [15], simulated annealing [16, 17] and gradient descent [15]. These algorithms tend to find the global optimum solution. However, they may be trapped temporarily in local optima. The local optima are sometimes nearly as important as the global one. In this paper, an algorithm has been used which specifies the global optimum as well as the local optima.

The optimization algorithm has three phases. During the first phase, the space of input variables is searched using a random basis method, and the fitness function is computed for each of these points. The fitness function determines the normalized single-mode bandwidth of each waveguide structure and it is defined as $\Delta\omega/\omega_0$, where ω_0 is the mid-frequency of the waveguide and $\Delta\omega$ specifies its frequency bandwidth. In the second phase, another algorithm receives these randomly generated input points and their respective fitness values, and estimates the whereabouts of the local maxima. In the final phase, for fine-tuning purpose, theses estimations are fed to a gradient algorithm for finding the exact values of the local maxima.

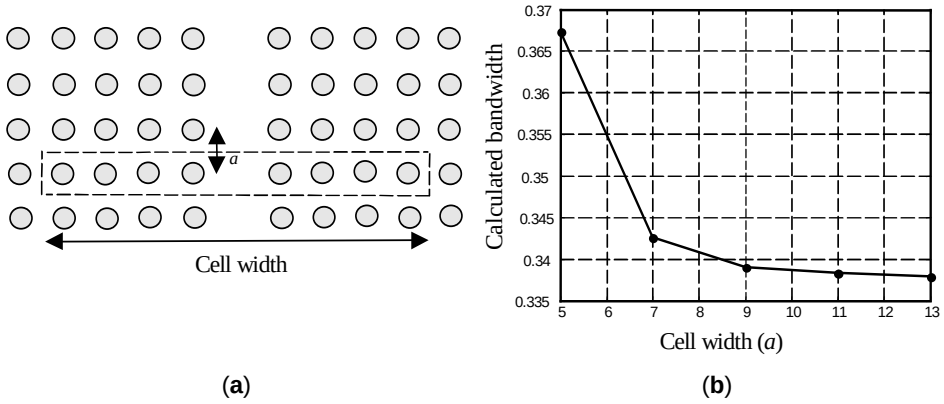

Fig. 1. A typical super-cell with a cell width of 9*a* in a square lattice of dielectric rods having a radius of 0.19*a* in which a column is omitted (**a**). Calculated normalized bandwidth for TM polarization *vs.* cell-width for the waveguide shown in Fig. 1**a** (**b**).

In order to use the PWE method for single-mode bandwidth calculation, a unit cell should be chosen [12]. Waveguides are periodic in one dimension, while the PWE method can only be used for structures that are periodic in two dimensions. To overcome this problem, we can use a super-cell, with a large cell-width, as shown in

Fig. 1**a**, and assume that the waveguide is periodic in two dimensions. Figure 1**b** illustrates the effect of cell-width on the calculated single-mode bandwidth of the waveguide shown in Fig. 1**a**. The dielectric is assumed to be GaAs with a dielectric constant of 11.4. The radius of the rods is 0.19a, where a is the lattice constant. Figure 1**b** shows that as the cell-width increases, the bandwidth approaches its final value (which is obtained when the cell-width tends to infinity). However, the error caused by the limited cell-width is negligible in the optimization process. For example, using a cell-width of 7a the calculated bandwidth still has two significant digits. In our calculations, the super cell dimension is chosen equal to 9a to guarantee less than 1% error. The flowchart of fitness calculation is demonstrated in Fig. 2. For a predefined unit cell with some geometrical input variables, a two dimensional dielectric constant matrix is constructed. Next, the discrete Fourier series of this matrix is calculated. Using all or the truncated form of this matrix, the PWE method is used to calculate the band diagram of the unit cell [19]. Finally, the normalized single-mode bandwidth (normalized to its mid-frequency) is calculated using the band diagram. This calculated value is provided in the output as the fitness value. Figure 3 depicts the band diagram of the structure shown in Fig. 1**a**. In this band diagram, the boundaries of single-mode region are represented by ω_1 and ω_2. Here the fitness value, defined as $\Delta\omega/\omega_0$, is equal to 33.8%.

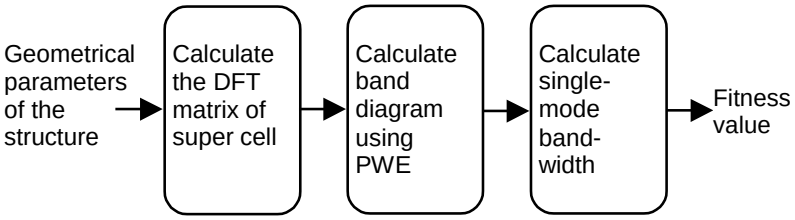

Fig. 2. The flowchart of fitness calculation.

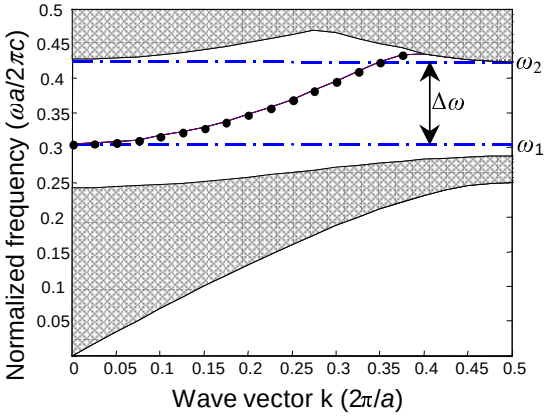

Fig. 3. The band diagram of the waveguide shown in Fig. 1**a**.

3. Optimization geometries

Among the conventional lattice configurations, square and triangular lattices are most commonly used. The waveguide structures that we consider for optimization and their corresponding unit cells are shown in Fig. 4. A super cell width of 9a is used for PWE analysis. As shown in Fig. 4, each structure has three optimization parameters. The first parameter (Var1) is related to the central region of the waveguide. The second parameter (Var2) is assigned to the adjacent rods that have a significant effect on the waveguide bandwidth. The third parameter (Var3) is the radius of other rods in the PC which determines the position and width of the bandgap. For TM polarization, the

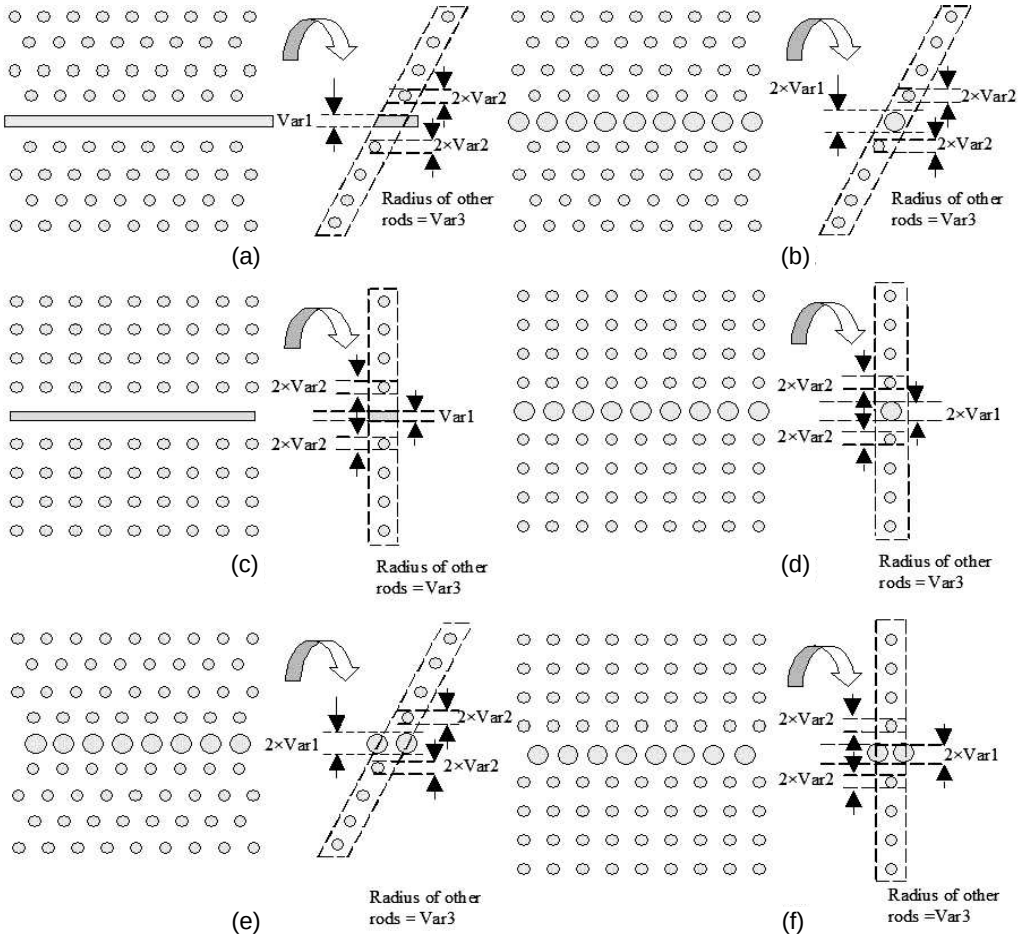

Fig. 4. Simulation parameters and the unit cell chosen for each case. Triangular lattice of dielectric rods combined with a dielectric strip (**a**), triangular lattice of dielectric rods (**b**), square lattice of dielectric rods combined with a dielectric strip (**c**), square lattice of dielectric rods (**d**), triangular lattice of dielectric rods with a row displaced half of the lattice constant (**e**), square lattice of dielectric rods with a row displaced half of the lattice constant (**f**).

gray parts of the structures shown in Fig. 4 are assumed to be GaAs with a dielectric constant of 11.4 and the background is assumed to be air. For TE polarization, the gray parts are assumed to be air and the rest is dielectric. Note that in Fig. 4, the diameter of rods (holes) is represented by 2 × Var1 and 2 × Var2, and the thickness of the strips (in Figs. 4**a** and 4**c**) is denoted by Var1.

Figure 4**a** is a combination of a triangular lattice of dielectric rods and a strip waveguide. Figure 4**b** is a triangular lattice of dielectric rods in which the radius of central rods is different. Part (**c**) depicts a square lattice of dielectric rods combined with a strip waveguide which has replaced the central row. Part (**d**) also shows a square lattice of dielectric rods in which the radius of the central row is chosen as an optimization parameter. In parts (**e**) and (**f**) a row has been shifted half of the lattice constant.

4. Increasing the waveguide bandwidth for TM polarization

All of the previously mentioned structures are optimized by the proposed algorithm to find the local and global maximums. The optimization corresponding to the structures shown in Fig. 4 are presented in Table 1. In this table, the first row of each section shows the fitness values. The second, third, and forth rows specify the values of Var1, Var2 and Var3, respectively. In each section, the second column corresponds to the global optimum and the following columns correspond to local optimums whose fitnesses are at least 70% of the global maximum. They are sorted in descending order of their fitness values. In fact, there exist much more local optimums which due to their poor fitness values are not listed in the table.

Table 1. Global and local maximums of fitness parameter obtained for the geometries shown in Fig. 4 and assuming TM polarization.

	Global Maximum	Local Max. 1	Local Max. 2	Local Max. 3
1	2	3	4	5
(a) Triangular lattice of dielectric rods combined with a dielectric strip				
fitness	0.412	0.407	0.402	0.342
Var1	0.20	0.15	0.31	0.04
Var2	0.21	0.18	0.25	0.20
Var3	0.20	0.16	0.24	0.21
(b) Triangular lattice of dielectric rods				
fitness	0.314	0.271	0.291	*
Var1	0.00	0.10	0.00	*
Var2	0.16	0.00	0.19	*
Var3	0.17	0.29	0.18	*
(c) Square lattice of dielectric rods combined with a dielectric strip				
fitness	0.380	0.344	*	*
Var1	0.20	0.00	*	*
Var2	0.20	0.20	*	*
Var3	0.20	0.19	*	*

1	2	3	4	5
(d) Square lattice of dielectric rods				
fitness	0.344	0.311	0.265	*
Var1	0.00	0.00	0.11	*
Var2	0.20	0.13	0.25	*
Var3	0.19	0.15	0.28	*
(e) Triangular lattice of dielectric rods with a row displaced half of the lattice constant				
fitness	0.348	0.300	0.255	*
Var1	0.06	0.10	0.10	*
Var2	0.16	0.24	0.00	*
Var3	0.17	0.22	0.31	*
(f) Square lattice of dielectric rods with a row displaced half of the lattice constant				
fitness	0.373	0.372	*	*
Var1	0.08	0.05	*	*
Var2	0.19	0.16	*	*
Var3	0.20	0.17	*	*

Table 1(a) illustrates the optimization results corresponding to the structure shown in Fig. 4**a**. It is interesting to mention that without the strip waveguide, the triangular lattice of dielectric rods does not provide a large single-mode bandwidth. In column 2, values of the geometrical variables corresponding to the global optimum are provided. It is important to note that the radius of rods for the global optimum of Table 1(a) is nearly the same as the commonly used radius of rods in a square lattice. Considering the fabrication and lithography resolution, the radii of the rods and the width of the strip waveguide have acceptable values.

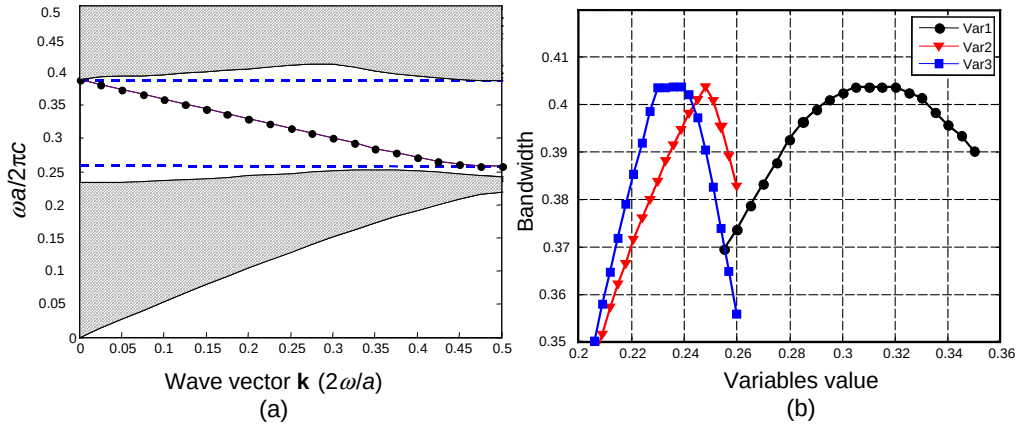

Fig. 5. Band diagram of the second local optimum in Table 1(a) (**a**) and its sensitivity curves (**b**).

An interesting result in Table 1(a) concerns the 2nd local maximum. Its fitness value is very close to the fitness of the global optimum, while the radius of PC rods is

0.24a instead of 0.2a, making it easier for implementation. The strip waveguide also has a width equal to 0.31a which is quite reasonable regarding the implementation concerns. Figure 5**a** shows the band diagram corresponding to this local optimum. As it can be seen, a wide-band single-mode geometry with approximately constant group-delay has been obtained. As shown in Fig. 5**a**, the guiding mode is located between frequencies 0.26(a/λ) and 0.39(a/λ) and so the normalized value of the single-mode bandwidth is equal to 40%. Each of the optimized variables is swept in the neighborhood of the optimum point while the remaining two variables are held constant to get a better overview of the proposed topologies sensitivities to the parameter variation. The results are presented in Fig. 5**b** as three sensitivity curves.

In Table 1(b), the fourth column shows another local optimum. This local optimum indicates that removing a single row (Var1 = 0) in a triangular lattice of dielectric rods provides a waveguide with fitness lower than the conventional TM waveguide realized in a square lattice of PC. This may be the main reason that for TM polarization most of the research has been dedicated to square lattices. The global maximum in Table 1(d) is very similar to the conventional choice which is recommended in the literature.

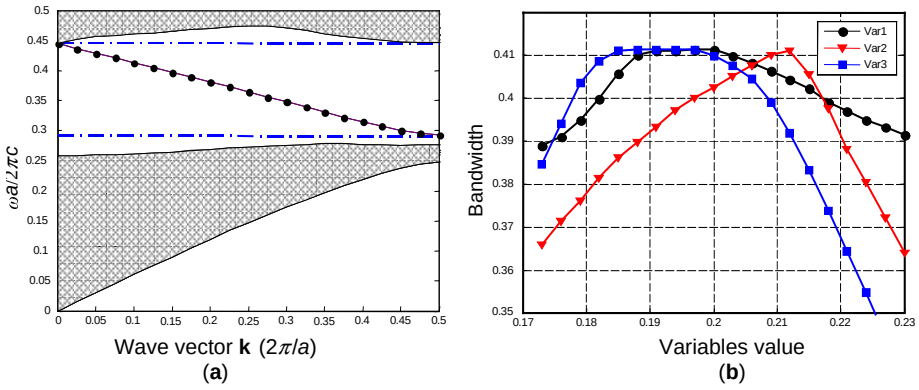

Fig. 6. (**a**) Band diagram for the global maximum of Table 1(a). (**b**) Its sensitivity curves.

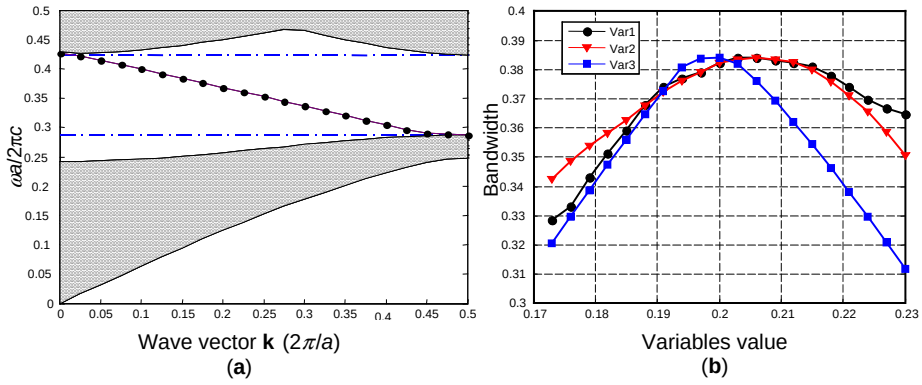

Fig 7. (**a**) Band diagram for the global maximum of Table 1(c). (**b**) Its sensitivity curves.

The overall maximum fitness is obtained for a triangular lattice of dielectric rods combined with a strip waveguide of Var1 = 0.2, Var2 = 0.21 and Var3 = 0.2 (global maximum in Table 1(a)). Figure 6**a** shows the band diagram of this global optimum waveguide. The normalized bandwidth of this waveguide is equal to 41.2%. Figure 6**b** illustrates the sensitivity curves related to the optimum waveguide presented in Table 1(a). It can be concluded from this figure that the fitness function variation is relatively low for small changes of the fabrication variables around their optimum values. As an example, for a 5% deviation in each variable, the values of fitness functions still remain above 40%. This gives some sort of robustness to the design. The fitness value obtained in this case (normalized bandwidth of 41.2%) is about 7% more than the fitness value of a conventional TM waveguide. The conventional waveguide for TM polarization is realized by removing a row in a square lattice of rods. This waveguide has a maximum single-mode bandwidth of 34.4%, as it can be seen in Table 1(d). Table 1(c) also provides a global maximum with a large fitness function value (38%) for the combination of a square lattice and a strip waveguide. Its band diagram and sensitivity curves are shown in Fig. 7**a** and Fig. 7**b**, respectively. Although Table 1(e) and Table 1(f) provide large bandwidths, they correspond to small feature sizes, which make them unsuitable from the implementation point of view.

5. Increasing the waveguide bandwidth for TE polarization

In order to obtain a wide-band waveguide for TE polarization, PCs with large bandgaps are needed. A triangular lattice of air holes in a dielectric environment can provide a large bandgap for TE polarization. For GaAs, the maximum bandgap occurs when the radius of PC holes is 0.45a. This makes the structure too fragile. Therefore, in most applications a radius of 0.3a is used instead. Conventional TE waveguides are realized by filling a single row in the above mentioned PC. ADIBI *et al.* tried to increase the bandwidth of conventional TE waveguides by optimizing the radii of the holes adjacent to the defect (see Fig. 8**a**) [11], [12].

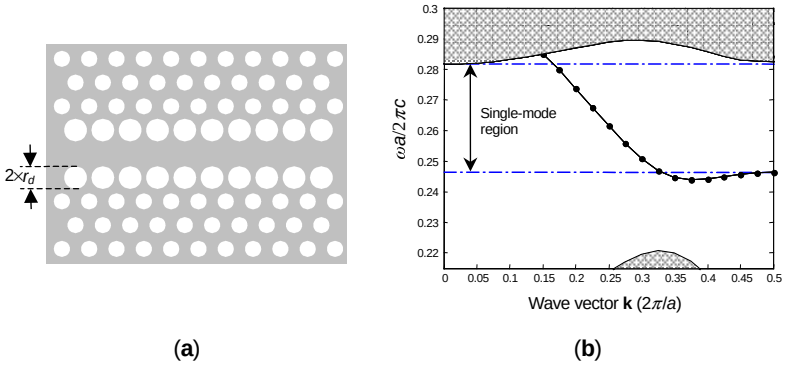

(**a**) (**b**)

Fig. 8. (**a**) The structure proposed in [11, 12], the gray part is dielectric with 11.4 dielectric constant while r_d = 0.42a and the radii of other holes are assumed to be 0.3a. (**b**) The resulting band diagram.

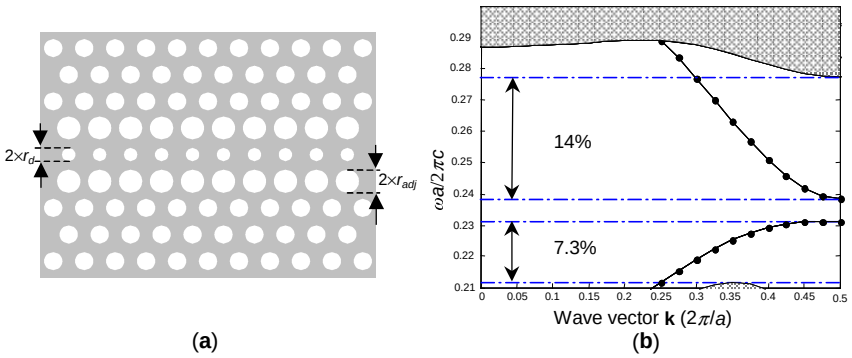

Fig. 9. The structure proposed in [14], the gray part is dielectric with 11.4 dielectric constant while r_d = 0.22a, r_{adj} = 0.38a and the radii of other holes are assumed to be 0.3a (**a**), the resulting band diagram (**b**).

Yamada *et al.* showed that shifting one row half of the lattice constant can also create a large bandwidth waveguide [13]. They optimized the radii of the shifted line defect to maximize the bandwidth. Combining the methods proposed in [11–13], the radii of the holes in line defect as well as the adjacent holes were optimized simultaneously to further increase the bandwidth. By this improvement, a normalized bandwidth of 21% can be obtained [14]. Figure 9 shows the structure proposed in [14] and its band diagram.

For TE polarization, rod type PCs do not provide large bandgaps. Hence, we choose the same geometries as in Fig. 4 for optimization, but in this case the gray sections of each structure are assumed to be air and the rest is dielectric. The optimization results are shown in Table 2. This table shows that the best results belong to parts (a) and (e), having bandwidths of 39.5% and 34.6%, respectively. Figures 10 and 11 show the band diagrams and sensitivity curves of these two waveguides, respectively.

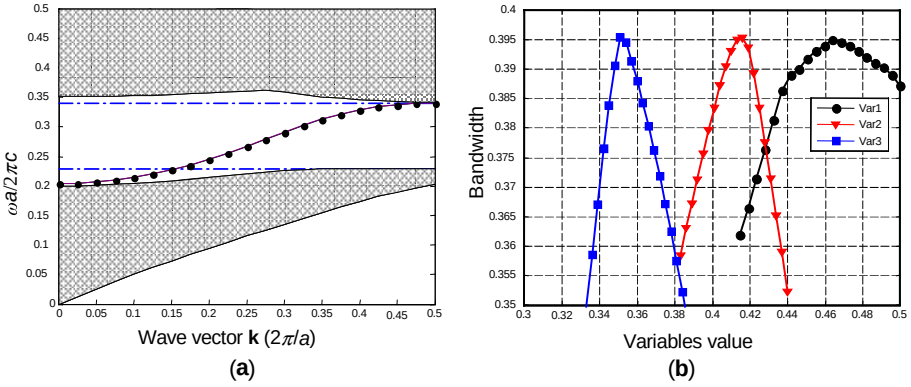

Fig. 10. The band diagram corresponding to the global maximum of Table 2**a** (**a**) and its sensitivity curves (**b**).

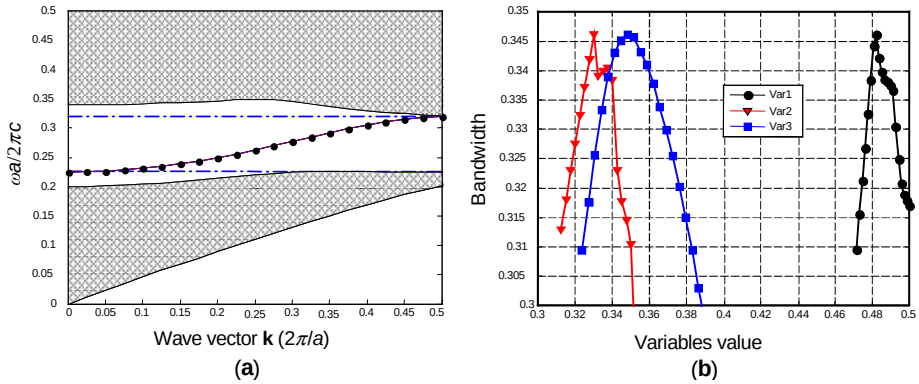

Fig. 11. The band diagram corresponding to the global maximum of Table 2(e) (**a**), and its sensitivity curves (**b**).

Table 2. Global and local maximums of fitness parameter obtained for the geometries shown in Fig. 4 and assuming TE polarization.

	Global Maximum	Local Max. 1	Local Max. 2	Local Max. 3
1	2	3	4	5
(a) Triangular lattice of dielectric air combined with an air strip				
fitness	0.395	0.269	*	*
Var1	0.45	0.29	*	*
Var2	0.42	0.36	*	
Var3	0.35	0.30	*	*
(b) Triangular lattice of air holes				
fitness	0.313	0.289	0.248	0.190
Var1	0.55	0.50	0.49	0.22
Var2	0.29	0.38	0.31	0.44
Var3	0.33	0.33	0.29	0.43
(c) Square lattice of air holes combined with an air strip				
fitness	0.106	0.101	*	*
Var1	0.47	0.04	*	*
Var2	0.42	0.41	*	*
Var3	0.40	0.39	*	*
(d) Square lattice of air holes				
fitness	0.104	0.104	0.101	0.086
Var1	0.20	0.04	0.49	0.25
Var2	0.44	0.39	0.43	0.49
Var3	0.43	0.38	0.43	0.39
(e) Triangular lattice of air holes with a row displaced half the lattice constant				
fitness	0.346	0.255	*	*
Var1	0.48	0.44	*	*
Var2	0.33	0.34	*	*
Var3	0.35	0.32	*	*

1	2	3	4	5
(f) Square lattice of air holes with a row displaced half the lattice constant				
fitness	0.111	0.110	0.108	*
Var1	0.45	0.03	0.12	*
Var2	0.41	0.42	0.45	*
Var3	0.41	0.41	0.41	*

Table 2(a) corresponds to a PC of triangular holes in a dielectric medium, from which a strip of dielectric has been removed. In the global optimum case, Var3 is equal to 0.35*a*, while for the local maximum it is equal to 0.3*a*. From the implementation point of view, the radius of 0.35*a* is not so large to make the structure fragile, but it can provide a bandwidth which is nearly double the one reported in [14]. The local maximum 1 in Table 2(a) has an optimum hole radius of 0.3*a*, which is equal to the hole radii used in [11–14], but its bandwidth is 5% greater than the best result reported in [14].

For the global optimum of Table 2(b), the radius of line-defect holes (Var1) has become so large that the holes join together and form a structure similar to Fig. 4**a**. Tables 2(c), 2(d) and 2(f) do not provide large bandwidth waveguides. The maximum bandwidth obtained in these cases does not exceed 11%. Table 2(e) is the optimization result of a triangular lattice of air holes, in which a row is displaced half of the lattice constant. The global and first local maximums of this structure provide single-mode bandwidth of 34.6% and 25.5%, respectively, while they have acceptable parameters.

6. Conclusions

A wide variety of PC waveguide structures has been investigated in order to obtain wide-band single mode TM and TE waveguides. All structures have been optimized using an algorithm that finds the global optimum as well as the local optimums. We have shown that in comparison with the global optimum, some local optimums can provide moderately wide bandwidths, while the radii of their holes/rods make the implementation easier. To our best knowledge, these local optimums are reported for the first time. For TM polarization, a single-mode waveguide with a bandwidth of 41% was proposed. This value is about 7% greater than the single-mode bandwidth of conventional TM waveguides. For TE polarization, a waveguide with 39% bandwidth was proposed. This bandwidth is nearly double the best result that has been reported in the literature.

References

[1] JOANNOPOULOS J.D., MEADE R.D., WINN J.N., *Photonic Crystals: Molding the Flow of Light*, Princeton Univ. Press, Princeton, 1995.

[2] NODA S., BABA T., *Roadmap on Photonic Crystals*, Kluwer Academic Publisher, 2003.

[3] MULOT M., SAYNATJOKI A., ARPIAINEN S., LIPSANEN H., AHOPELTO J., *Photonic crystal slabs with ring-shaped holes in a triangular lattice*, 7th International Conference on Transparent Optical Networks (ICTON), Barcelona, Spain, 2005, pp. 155–58.

[4] ZALEVSKY Z., RUDNITSKY A., NATHAN M., *Nano photonic and ultra fast all-optical processing modules*, Optics Express, **13**, 2005, pp. 10272–284.

[5] SHINYA A., TAKARA H., KAWANISHI S., *All-optical flip-flop circuit composed of coupled two-port resonant tunneling filter in two-dimensional photonic crystal slab*, Optics Express, **14**, 2006, pp. 1230–35.

[6] MIAO B., CHEN C., SHARKWAY A., SHI S., PRATHER D.W., *Two bit optical analog-to-digital converter based on photonic crystals*, Optics Express, **14**, 2006, pp. 7966–73.

[7] NODA S., IMADA M., OKANO M., OGAWA S., MOCHIZUKI M., CHUTINAN A., *Semiconductor three-dimensional and two-dimensional photonic crystals and devices*, IEEE Journal of Quantum Electronics, **38**, 2002, pp. 726–35.

[8] NIELSEN J.B., SONDERGAARD T., BARKOU S.E., BJARKLEV A., BROENG J., *Two-dimensional Kagome structure fundamental hexagonal photonic crystal configuration*, IEEE Electron Letters, **35**, 1999, pp. 1736–37.

[9] NIELSEN J.B., SONDERGAARD T., BARKOU S.E., BJARKLEV A., BROENG J., *Two-dimensional Kagome photonic bandgap waveguide*, IEEE Photonics Technology Letters, **12**, 2000, pp. 630–632.

[10] JOHNSON S.G., VILLENEUVE P.R., FAN S., JOANNOPOULOS J.D., *Linear waveguides in photonic-crystal slabs*, Physical Review, B, **62**, 2000, pp. 8212–22.

[11] ADIBI A., LEE R.K., XU Y., YARIV A., SCHERER A., *Design of photonic crystal with single-mode propagation in photonic bandgap*, IEEE Electron Letters, **36**, 2000, pp. 1376–78.

[12] BADIEIROSTAMI M., MOMENI B., SOLTANI M., ADIBI A., *Investigation of physical mechanisms in coupling photonic crystal waveguiding structures*, Optics Express, **12**, 2004, pp. 4781–89.

[13] YAMADA K., MORITA H., SHINYA A., NOTOMI M., *Improved line-defect structures for photonic-crystal waveguides with high group velocity*, Optics Communication, 2001, pp. 395–402.

[14] KHATIBI MOGHADAM M., *Design and Analysis of Photonic Crystal Structures*, M. Sc. Thesis, Electrical Engineering Department, Ferdowsi University of Mashhad, 2006.

[15] REEVES C.R., ROWE J.E., *Genetic Algorithms Principles and Perspectives: A Guide to GA Theory*, Kluwer Academic Publishers, 2003.

[16] AARTS E.H.L., KOARST J., *Simulated Annealing and Boltzmann Machines: A Stochastic Approach to Combinatorial Optimization*, Wiley, Chichester, New York, 1989.

[17] LAARHOVEN P.J.M., AARTS E.H.L., *Simulated Annealing: Theory and Applications*, Kluwer Academic Publishers, 1987.

[18] JANG J.-S.R., SUN C.-T., *Neuro-Fuzzy and Soft Computing: A Computational Approach to Learning and Machine Intelligence*, Prentice-Hall, Upper Saddle River, NJ, 1996.

[19] GUO S., ALBIN S., *Simple plane wave implementation for photonic crystal calculations*, Optics Express, **11**, 2003, pp. 167–75.

Received March 3, 2008